Engineering Fracture Mechanics 210 (2019) 444–451

Contents lists available at ScienceDirect

Engineering Fracture Mechanics

journal homepage: www.elsevier.com/locate/engfracmech

Acoustic emission investigation of the effect of graphene on the fracture behavior of cement mortars

Ilias K. Tragazikis, Konstantinos G. Dassios, Panagiota T. Dalla, Dimitrios A. Exarchos, Theodore E. Matikas*

Department of Materials Science and Engineering, University of Ioannina, Dourouti University Campus, Ioannina GR-45110, Greece

A B S T R A C T

Graphene-modified cements are envisioned as next-generation multifunctional construction materials with superior mechanical performance and smart strain sensing capabilities. The presence study aims to fill the current lack of knowledge on the effect of graphene presence on the fracture behavior and mechanical response of nanoplatelet-modified mortars. Pure bending, compression and fracture tests with simultaneous AE monitoring were carried out on specimens fabricated by introduction of pure few-layer graphene nanoplatelets in the mixture by aid of a superplasticizer doubling as surfactant. The nanoplatelets were found responsible for dramatic improvements of the order of 1700% in the fracture energy requirements of the mortars. The improvements were independently validated by acoustic emission data which also highlighted the very high energy dissipation potential of graphene nanoplatelets which endowed ductility to the highly-brittle plain material and indicated a shift in the fracture mode of the mortars from shear to tensile attributed exclusively to platelet presence.

1. Introduction

As the primary constituent in the production of concrete, Ordinary Portland cement (OPC) is the single most widely used construction material in the world. OPC's major disadvantages are its inherent brittleness, which is responsible for a low cracking resistance, its low tensile strength due to internal flaws and its poor strain capacity. Such limitations can be overcome by embedment, in the material bulk, of reinforcing phases of either macro-dimensions, such as steel bars, or of micro-scale ones, such as fibers, which can endow tensile strength to the material and improve its cracking resistance and damage tolerance through apportionment of the applied load to the ductile reinforcements but also through the development of energy dissipation mechanisms such as bridging and pull-out [1].

Recent advances in nanotechnology have highlighted nano-scale materials such as nano-silica particles and carbon nanotubes (CNTs), as promising candidate reinforcements for next-generation cement composites with not only improved mechanical performance, but also with multi-functional features such as thermal and electrical transport potential [2]. Owing to their exceptional mechanical properties, high strength and stiffness, CNTs are significantly advantageous for cement reinforcement compared to conventional fibers while, as one-dimensional materials of high aspect ratio, they can effectively inhibit crack initiation and propagation by consuming energy which is correspondingly deprived from the fatal work of crack growth [3].

Graphene, the single-atom-thick flat sheet consisting, similarly to CNT walls, of hexagonal lattices of sp^2-bonded carbon atoms, exhibits equally exotic mechanical performance as the tubes, with reported tensile strengths and elastic moduli reaching 130 GPa and

* Corresponding author.
E-mail address: matikas@cc.uoi.gr (T.E. Matikas).

https://doi.org/10.1016/j.engfracmech.2018.01.004
Received 7 November 2017; Received in revised form 10 January 2018; Accepted 10 January 2018
Available online 11 January 2018
0013-7944/

1 TPa, respectively [4]. Graphene is hierarchically superior to CNTs as also indicated by the mere definition of the tubes as graphene sheets rolled into seamless hollow cylinders [5]. Due to the planar morphology of the nanoplatelets, which allows attainment of contact areas with the continuous medium as high as 2630 m^2/g [6], double of the contact area offered by CNTs, graphene can generate more sites for potential chemical or physical bonding with the host material, hence potentially outperforming the tubes in terms of reinforcement [3]. Analogously, much smaller graphene content may be required to match the mechanical performance enhancement offered by nanotubes [7]. Embedment of graphene nanoplatelets in cement is envisaged as the plausible way towards development of next-generation smart multifunctional construction composites with superior mechanical performance and strain sensing capabilities.

Due to the complexity and high costs associated with synthesizing high quality nanoplatelets, research on graphene-modified cement is currently in its infancy with the first remote mentions dating in 2013 and 2014 [7,8] and a handful of relevant publications since. A less expensive and easier to synthesize graphene derivative, graphene oxide (GO), has been investigated for the mechanical reinforcement [3,9,10] and endowment of transport potential to cement [11]. GO, consisting of sp^2-hybridized carbon atoms, has satisfactory strength and dispersibility in aqueous solutions, but the inherent defects in its lattice are responsible for its significantly low strength and inferiority compared to graphene [12]. As a result, there is currently a wide lack of knowledge on the degree of improvement of the mechanical properties that pure graphene can potentially offer to cement. Specifically, to the authors' knowledge, the extremely scarce information in the literature on the effect of graphene presence on the flexural or compressive behavior of cement is almost exclusively limited to the paste form of the material [3,13–15], with the only exception being [16] where mortars are tested for flexural strength determination under three point (mixed) bending. Moreover, there is currently complete lack of bibliographical mention of the effect of graphene on the fracture behavior of cement which is of primary importance for the structural applications employing cement-based materials.

The present paper aims to fill the current knowledge gap by providing useful insight on the effect of graphene presence on the mechanical and fracture behavior of graphene-modified mortars. For this task, pure bending tests, compressive and fracture tests with simultaneous acoustic emission monitoring were carried out on specimens fabricated by introduction of the nanoplatelets via the mixing water by aid of a superplasticizer doubling as surfactant. The mechanical response of the material is discussed in view of the particularities in graphene morphology whereas fracture energy and acoustic emission indices are used to evaluate the effect of nanoplatelet content in the energy dissipation potential of the material. The fracture mode of the graphene-modified cements is revealed by AE descriptors and discussed.

2. Experimental procedure

2.1. Materials

A total of three cement mixtures, at graphene concentrations of 0.2 and 0.4 wt% of cement and a reference mixture without graphene were prepared for investigation of the effect of nanoplatelet presence on the mechanical and fracture properties of the material. At each graphene content level, sets of six prismatic specimens of dimensions of 40 × 40 × 160 mm^3 were prepared and apportioned equally for three- and four-point bending tests. Mixtures contained ordinary Portland cement type I 42.5t, regular tap water, natural sand and dry powders of extremely fine and pristine graphene nanoplatelets commercially available as Pure Graphene Plus™ by Directa Plus SpA (Como, Italy). Table 1 summarizes the main properties of the nanoplatelets; their nominal thickness indicates a high-quality few-layer pristine material. A water-based superplasticizer of polycarboxylate polymers, namely Viscocrete Ultra 300 superplasticizer (Sika AG, Baar, Switzerland), was used as graphene dispersant agent at a 1.5/1 weight ratio to graphene. As introduced in [17], usage of such a native cement additive not only provides high homogenization quality but also renders employment of conventional dispersion methods, such as surfactant usage and chemical functionalization methods, completely unnecessary. The efficiency of superplasticizers as nanoplatelet dispersant agents for exfoliated graphene-cement composites has also been discussed in [18]. In every mixture, a small amount of Viscocrete Ultra 600 superplasticizer, with similar characteristics to Viscocrete Ultra 300, was also used to maintain the workability of the fresh mortar at acceptable levels. The particular superplasticizers were selected based on their efficiency in preventing air entrapment in the material as well as due to their excellent resistance to mechanical and chemical attack. Water to cement ratio was maintained at 0.5.

Table 1
Properties of Pure Graphene Plus nanoplatelets used.

Property	Value
Carbon content	> 97 wt%
Oxygen content	< 0.6 wt%
Sulphur content	< 0.2 wt%
Apparent density	60 g/L
pH	5–7
Lateral dimension	< 10–15 μm
Thickness	< 2–4 nm

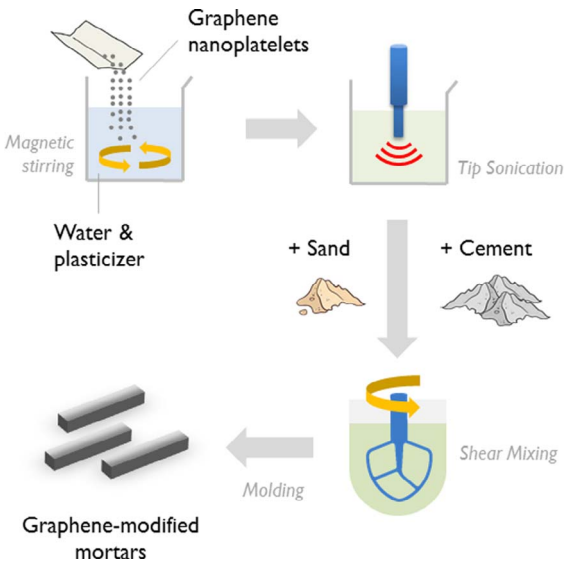

Fig. 1. Schematic representation of the step in the manufacturing process for graphene-modified mortars.

2.2. Preparation of nano-modified mortars

The experimental procedure for the preparation of graphene-modified cement mortars is presented schematically in Fig. 1. It consisted of the following steps: Initially, aqueous graphene suspensions were produced by addition of nanoplatelets – at weights inscribed by the desirable target contents in the resultant materials – in mixtures of regular tap water and plasticizer and subsequent magnetic stirring for 2 min. The suspensions were homogenized by ultrasonication for 90 min at room temperature, using a Hielscher UP400S device (Hielscher Ultrasonics GmbH, Teltow, Germany) equipped with a cylindrical Ø22 mm sonotrode delivering a power throughput of 4500 J/min at a frequency of 24 kHz. The specific combination of energy rate and sonication duration was established as optimum following a meticulous investigation of the effect of ultrasonication parameters of suspension quality [19]. The suspensions were subsequently processed under vacuum for complete removal of entrapped air prior to mixing with cement and sand. Reference mixtures without graphene nanoplatelets were also prepared for comparison purposes. The vacuumed suspensions were transferred, along with ordinary Portland cement and natural sand into the bucket of the laboratory rotary mixer where they were mixed, in low and high speeds sequentially, for a total duration of 4 min according to requirements of standard test method BS EN 196-1. Immediately after, the fresh mortars were poured into oiled steel moulds with inner dimensions of $40 \times 40 \times 160\ mm^3$ and were left to harden for 24 h before demolding. They were subsequently placed in the 100% humidity room for curing for a duration of 28 days. Bending specimens were produced after machining of notches, length 20 mm, in the cured mortars by means of a cut-wheel.

2.3. Mechanical testing and non-destructive characterization

2.3.1. Bending and compressive test

Mechanical testing of mortars for the characterization of their pure bending strength under the four-point bending configuration and of their compressive strength was carried out on an Instron 5967 frame (Instron, Norwood, MA, USA) equipped with a 30 kN loadcell following standard test method ASTM C1609. For each graphene content, three prismatic specimens were catastrophically tested under crosshead displacement control at a speed of 0.01 mm/s. The latter value was selected as optimal for allowing attainment of the maximum load within a duration of 30–60 s from the start of the test. Following catastrophic failure, the two halves of failed prisms were subjected to compressive loading, at a load rate of 2400 N/s, equivalent to a stress rate of 1.5 MPa/s for the $40 \times 40\ mm^2$ cross sectional areas, for the characterization of compressive strength as per standard protocol EN 196-1:2005.

2.3.2. Fracture energy measurements

Characterization of the fracture behavior of the graphene-modified mortars under three point bending with simultaneous acoustic emission monitoring as presented in the schematic of Fig. 2, was performed on the same testing frame as pure bending. Crack mouth opening displacement (CMOD) was measured within a central gauge length of 10 mm using an Instron™ clip gauge mounted on knife-edges. Pair values of (CMOD, load) were recorded continuously up to the point where the beams were completely separated into two halves. The accuracy of the load measurements in the test was at least 2% of the maximum load level while the CMOD was measured with an accuracy of at least 0.01 mm. The measured CMOD was corrected to account for the distance of the measurement point from the notch mouth, which is defined by the thickness of the clip gauge knife edges, *d*. The correction enabling the determination of the true CMOD value is given by Eq. (1) [20]:

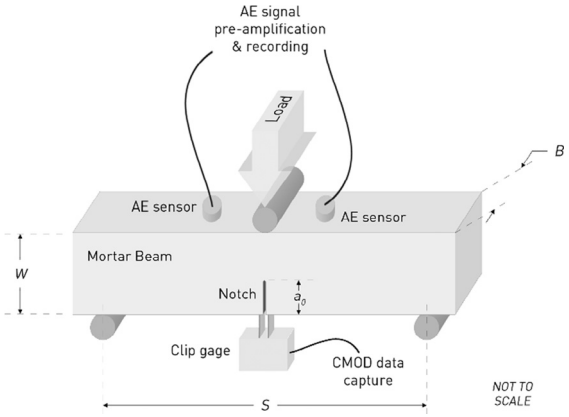

Fig. 2. Three-point bend testing configuration for fracture testing of cement-modified mortarts with simultaneous acoustic emission monitoring.

$$\mathrm{CMOD} = \mathrm{k_d CMOD^{Measured}} \tag{1}$$

where $\mathrm{CMOD^{Measured}}$ is the measured value and $\mathrm{k_d}$ is the conversion factor which, for most knife edge thicknesses, can be determined using Eq. (2) [20].

$$K_d(d,a) = \frac{h_1 + h_2 a}{1 + h_3 a + h_4 a^2} \tag{2}$$

The values of coefficients h_i used to compute $\mathrm{k_d}$ for a knife-edge thickness of 3 mm relevant to the clip gauge of this study, are given in Table 2 [20].

Fracture energy, $\mathrm{G_f}$ (SI units of N/m or $\mathrm{J/m^2}$), is defined as the amount of energy necessary to create one unit area of crack which, in turn, is defined as the projected area on a plane parallel to the main crack direction. It can be determined from the area under the load-CMOD curve, $\mathrm{W_0}$, by Eq. (3) [20]:

$$G_F = \frac{W_0 + mg\delta_0}{A_{lig}} \tag{3}$$

where g is the gravitational acceleration, δ_0 is the CMOD of the beam at fracture and A_{lig} is the area of the ligament defined as the projection of the fracture zone on a plane perpendicular to the beam axis given by:

$$m = m_1 + 2m_2 \tag{4}$$

where m_1 is the weight of the beam between the supports, calculated as the beam weight multiplied by the ratio of beam span over beam length, S/L and m_2 is the weight of the part of the loading device touching the beam which is not attached to the testing machine, but follows the beam until fracture. The lengths L and S were measured with an accuracy of < 0.5 mm.

2.4. Acoustic emission monitoring

During three point bending tests, the acoustic emission activity of the specimens was monitored continuously on the solid's surface by piezoelectric transducers. The latter transform the energy of the collected transient elastic waves, stemming from localized damage events in the material, to electric waveforms which are digitally collected and stored for subsequent analysis. Key parameters in a typical AE waveform are the amplitude (A), which is the maximum voltage of the AE signal measured in decibels (dB), the threshold, a user-defined amplitude value in dB based on background noise level, the rise time (RT) which is the time between the first threshold crossing and maximum peak amplitude, AE counts, corresponding to the number of times an AE burst crosses the threshold, RA, defined as the ratio of rise time over amplitude (RT/A), AE duration which is the time between the first and last threshold crossing and AE energy which is the area under the amplitude–time curve above the threshold value. The number of AE counts divided by the duration of the signal corresponds to the average frequency (AF, kHz); the index is useful in the classification of the fracture mode of the material, in either tensile or shear. As shear cracks appear first during damage accumulation in the material with tensile ones following, characterization of the cracking mode can provide early failure warnings. Additionally, tensile events are linked to higher frequency content and higher RA values, than shear events [21].

Table 2
Coefficients used to compute $\mathrm{k_d}$ for the CMOD correction.

h1	h2	h3	h4
0.1037	104.1	105.1	0.01631

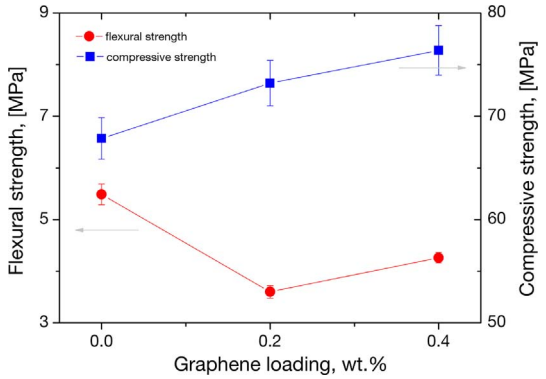

Fig. 3. Variation of flexural and compressive strength of graphene-modified mortars as a function of graphene nanoplatelet content.

During three point bending tests of graphene-modified mortars, AE activity was monitored using two R15a AE sensors (Physical Acoustics Corp, Princeton, New Jersey, USA), attached on the upper (un-notched) side of mortar beams at a distance of 40 mm as depicted in Fig. 2. The sensors had a sensitivity response ranging from 50 to 400 kHz and a maximum sensitivity at 150 kHz. The pre-amplifier gain was set at 40 dB while the signals were recorded on a dedicated PCI-2 board (Physical Acoustics Corp, Princeton, New Jersey, USA). To exclude external sources like noise from the loading points, AE localization was enabled and the threshold was set at 45 dB.

3. Results

3.1. Mechanical performance

The effect of graphene content on the flexural and compressive strength of nanoplatelet-modified mortars is plotted in Fig. 3. It is primarily observed that graphene presence in the mortars decreases their flexural strength under four point bending, with the strengths of mortars with 0.2 and 0.4 wt% of cement graphene nanoplatelets appearing lower by 42% and 27%, respectively, compared to control specimens. On the other hand, a continuous monotonic increase of the compressive strength of the mortars was noted with graphene content. A maximum improvement of 13% compared to control specimens was noted for the highest graphene content, 0.4 wt% of cement; the corresponding increase in compressive strength for specimens with 0.2 wt% content, was 8%.

The observed variation of flexural and compressive strength with nanotube content can be rationalized by consideration of graphene's particular morphology. As flake-shaped carbon atom lattices, the nanoplatelets distributed at random orientations inside the mortars offer planar reinforcement by accommodating part of the externally applied bending stress. However, based on reinforcement theory fundamentals, only the portion of nanoplatelets lying on planes parallel to the beam's neutral plane fully contributes to reinforcement, as no transverse stresses develop under pure bending. Off-axis platelets contribute less to the phenomenon as the angle of orientation with respect to the beam's neutral axis increases. The portion of nanoplatelets oriented perpendicular to the beam's neutral plane does not contribute to reinforcement at all. On the contrary, under the action of pure bending moments of four point bending, presence of such vertical nanoplatelets can locally interrupt the continuity of the bulk cement matrix and affect the stress transfer process along the beam axis. Provided the interphase between the matrix and graphene is moderately weak, as anticipated by a coarse bulk phase and a nanoscale reinforcement, this can lead to microcrack formation, hence also decreased flexural strength. The decrease documented herein does not agree with the only relevant mention of flexural strength of graphene-modified mortars available in the literature [16], where an improvement of 34% in the property is quoted for a nanoplatelet content of 0.02 wt% of cement. It must be emphasized however that, as opposed to the pure bending state applicable in the four-point tests of the present work, the literature value was obtained under three-point flexure where mixed bending conditions apply where both shear and tension act synergistically. In three point bending, peak stress localization occurs at the middle contact point and the test is standard practice mainly for fracture testing. The four point flexure test yields peak stresses along an extended area of the material hence a statistically larger portion with higher possibility of potential defects and flaws is interrogated.

Under the action of axial compressive forces, previously perpendicularly-oriented graphene flakes are now lying along the direction of load and can accommodate the axial deformation, hence contributing to superior compressive strength. The angle of orientation of the nanoplatelets has an opposite effect on compressive strength compared to the flexural. Here, only the portion of nanoplatelets lying on planes perpendicular to the beam's neutral plane fully contribute to reinforcement while off-axis platelets contribute less as the angle of orientation with respect to the beam's axis increases. However, contrary to flexure, the portion of nanoplatelets oriented perpendicular to the beam's compression axis, does not incur problems to the stress transfer process as the compression of flakes does not interrupt material coherence nor can it induce matrix micro-cracking. The maximum increase of 13% in compressive strength observed herein compares well with the corresponding improvement, in the vicinity of $< 20\%$ quoted for a graphene content of 0.02 wt% in the reference study [16].

The variation of fracture energy released during three-point bending of the graphene-reinforced mortars, is plotted together with acoustic emission energy as a function of graphene content in Fig. 4. Therein, an impressive improvement in the fracture energy of

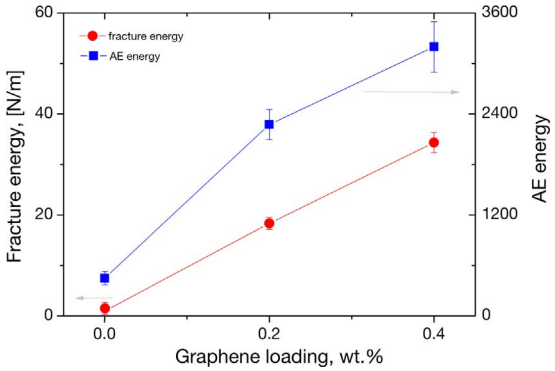

Fig. 4. Acoustic emission and fracture energy variation with graphene content during flexural testing of mortars.

the mortars as a result of graphene presence is observed. The amount of fracture energy associated with mortars modified with 0.2 wt % graphene was found increased by ca. 1400% compared to control specimens whereas the improvement reached ca. 1700% at graphene contents of 0.4 wt%. This finding demonstrates an extreme potential of graphene nanoplatelets in drastically improving the overall fracture behavior of mortars.

The variation of AE energy, representing the energy released during the flexural test, is also helpful in characterizing the fracture behavior of the material as the property is related to the material's fracture toughness [22]. Corresponding significant increases of 250% and 400% in AE energy compared to the control values were noted for mortars with 0.2 and 0.4 wt% graphene contents, respectively. Moreover, the monotonic rise trend of AE energy was observed to be almost identical to that of fracture energy. This observation is extremely significant because fracture energy and AE energy are two completely independent fracture indices relying on different physical phenomena; their agreement inarguably validates the dramatic impact of graphene presence on the material's fracture properties.

For conception of the effect of graphene nanoplatelet concentration on the nanoplatelet-modified materials' mechanical response, the temporal load variation during three-point bending tests of the mortars is plotted together with instant acoustic emission activity in Fig. 5. For comparison purposes, all axes are plotted in common ranges throughout contents. Several observations can be made by

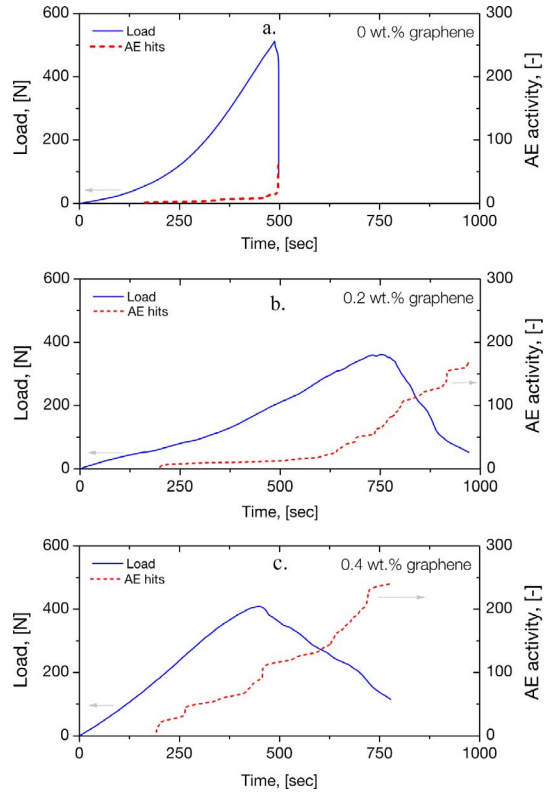

Fig. 5. Typical load and AE activity variation during three point bending of mortars modified with different concentration of graphene nanoplatelets.

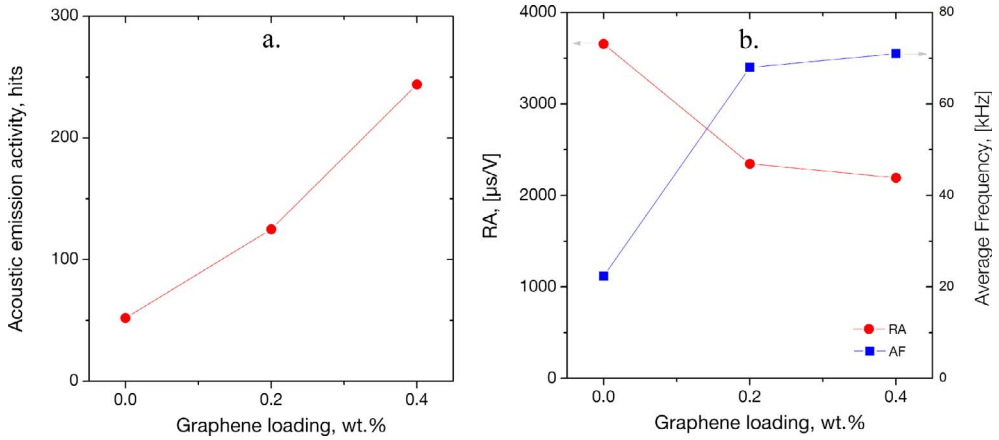

Fig. 6. Variation of the average RA value and average frequency as a function of graphene concentration in the mortars.

investigation of Fig. 5. A first observation concerns the limited amount of acoustic emission activity prior to the attainment of the maximum load, independently of graphene content. This is not unanticipated behavior as no microcracking phenomena which could give rise to AE activity are expected in the material in the early loading stages. Secondarily, the trend of load variation with testing duration appears highly dependent on graphene presence. Specifically, the behavior of plain mortars appears typically brittle, with a linear-elastic response up to failure which occurs immediately after the assumption of the maximum load. There is complete absence of energy dissipation phenomena in these mortars. A completely different picture is seen in graphene-modified mortars where the curves exhibit long "tails" after attainment of the maximum load, a behavior typical of a more ductile response. Such behavior stems from energy dissipation mechanisms developing and acting around the embedded graphene nanoplatelets; possible mechanisms include crack splitting and deflection at graphene locations but also load-sharing by stretching of the nanoplatelets, crack bridging by intact nanoplatelets and pull-out of failed ones. The existence of such phenomena is supported by a third observation, which concerns the presence of significantly high AE activity in the post-maximum load regimes of nanoplatelet-modified mortars. Recalling that AE sensors record events until specimens are completely separated in two halves, such activity signifies the existence of progressively severe failure phenomena after matrix cracking, which increase the fracture energy requirements of the material and can be attributed exclusively to graphene presence.

The energy dissipation potential of graphene in the mortars, which is responsible for the dramatic improvement in the material's fracture behavior, can be highlighted by consideration of the variation of the acoustic emission activity in the mortars, which is representative of the amount of damage events in the material, Fig. 6a. Therein, the amount of acoustic emission activity is observed to increase monotonically with graphene concentration in the mixture with improvements of 400 and 600% documented for mortars loaded with 0.2 and 0.4 wt% graphene nanoplatelets, respectively. This finding signifies that introduction of more nanoplatelets provides a greater population of locations available for energy dissipation by crack splitting and deflection, crack bridging and pull-out. Similar AE activity patterns have been documented for carbon nanotube-modified mortars under bending [23].

To assess the effect of graphene nanoplatelet content on the mortar's fracture mode, two key AE descriptors are invoked, namely average RA (ratio of rise time over amplitude) and AF (average frequency: ratio of number of AE counts over signal duration). Shear and tensile fracture modes are known to be linked to specific AF and RA values observation [17]. In three point bending tests, higher RA values in the vicinity of 4000 μs/V indicate shear fractures, whereas RA values near 2000 μs/V indicate tensile fracture modes. RA and AF values of the mortars in the present study are plotted as functions of graphene content in Fig. 6b. Therein, the addition of 0.2 wt% graphene in the mortars is observed to result in a decrease of the reference value of ca. 3500 μs/V (plain specimens) to ca. 2500 μs/V for 0.2 wt%-graphene-loaded mortars and to ca. 2000 μs/V for 0.4 wt%-loaded ones. This indicates that graphene presence is responsible for a shift in the fracture mode of the mortar from the shear state of in plain specimens, to tensile.

AF variation is also indicative of potential fracture mode shifts. With AF values in the vicinity of 30 kHz indicating shear failure and values near 60 kHz indicating tensile ones [24], the values of 25 and 70 kHz established for plain and 0.4 wt% graphene loaded mortars, respectively (Fig. 6b) confirm a clear change in mode of fracture of the mortars due to graphene nanoplatelet presence. The improvement in fracture energy as a result of graphene presence is linked to the observed shift of fracture mode from shear to tensile, through the superior behavior of graphene in tension than in shear, as indicated by the corresponding nominal strengths of approximately 610 MPa and 12 GPa, respectively [25].

4. Conclusions

The effect of pure few-layer graphene nanoplatelet presence, on the mechanical and fracture response of cement mortars was investigated herein by pure bending, compression and three-point bending tests with simultaneous AE monitoring. The observed changes in the flexural and compressive strengths of the mortars were rationalized upon the effect of nanoplatelet orientation in the bulk material which, respectively, either promotes microcracking or efficiently accommodates the imposed stress level. Nanoplatelet

presence was responsible for impressive improvements in the fracture behavior of the mortars with documented fracture energies up to 1700% higher than control values for graphene contents of 0.4 wt% of cement. The improvements were independently validated by acoustic emission energy measurements which showed monotonic rise trends, with respect to nanoplatelet content, almost identical to that of fracture energy. The particular finding is highly significant because fracture and acoustic emission energies are completely uncorrelated indices relying on different physical phenomena. Acoustic emission activity also revealed the effectiveness of graphene in endowing energy dissipation characteristics to the otherwise highly-brittle material by increasing its fracture energy requirements; possible mechanisms include crack splitting and deflection at nanoplatelet locations, load-sharing by stretching of nanoplatelets, crack bridging by intact graphenes and pull-out of failed graphenes from the cement bulk. The RA acoustic emission index revealed that graphene presence is also exclusively responsible for the shift in the fracture mode of the mortars from shear to tensile.

Acknowledgement

The authors wish to thank Prof. Costas Galiotis, Dept. of Chemical Engineering, University of Patras, Greece and George Trakakis, PhD, Institute of Chemical Engineering Sciences, Foundation for Research and Technology Hellas, for providing the pure graphene nanoplatelets used in the current research.

References

[1] Kang J, Kim K, Lim YM, et al. Modeling of fiber-reinforced cement composites: discrete representation of fiber pullout. Int J Solids Struct 2014;51(10):1970–9.
[2] Dalla PT, Dassios KG, Tragazikis IK, et al. Carbon nanotubes and nanofibers as strain and damage sensors for smart cement. Mater Today Commun 2016;8:196–204.
[3] Pan Z, He L, Qiu L, et al. Mechanical properties and microstructure of a graphene oxide-cement composite. Cem Concr Compos 2015;58:140–7.
[4] Lee C, Wei X, Kysar JW, et al. Measurement of the elastic properties and intrinsic strength of monolayer graphene. Science 2008;321:385.
[5] Kaushik BK, Majumder MK. Carbon nanotube: properties and applications. New Delhi: Springer India; 2015.
[6] Peigney A, Laurent C, Flahaut E, et al. Specific surface area of carbon nanotubes and bundles of carbon nanotubes. Carbon 2001;39(4):507–14.
[7] Rafiee MA, Lu W, Thomas AV, et al. Graphene nanoribbon composites. ACS Nano 2010;4(12):7415–20.
[8] Alkhateb H, Al-Ostaz A, Cheng AH-D, et al. Materials genome for graphene-cement nanocomposites. J Nanomech Micromech 2013;3(3):67–77.
[9] Chuah S, Pan Z, Sanjayan JG, et al. Nano reinforced cement and concrete composites and new perspective from graphene oxide. Constr Build Mater 2014;73:113–24.
[10] Lv S, Ma Y, Qiu C, et al. Effect of graphene oxide nanosheets of microstructure and mechanical properties of cement composites. Constr Build Mater 2013;49:121–7.
[11] Mohammed A, Sanjayan JG, Duan WH, et al. Incorporating graphene oxide in cement composites: a study of transport properties. Constr Build Mater 2015;84:341–7.
[12] Zhu Y, Murali S, Cai W, et al. Graphene and graphene oxide: synthesis, properties, and applications. Adv Mater 2010;22(35):3906–24.
[13] Effect of graphene on mechanical properties and microstructure of cement paste. Harbin Gongye Daxue Xuebao/J Harbin Inst Technol 2015;47(12):26–30.
[14] Metaxa ZS. Exfoliated graphene nanoplatelet cement-based nanocomposites as piezoresistive sensors: influence of nanoreinforcement lateral size on monitoring capability. Cien Tecnol Mater 2016;28(1):73–9.
[15] Wang B, Jiang R, Wu Z. Investigation of the mechanical properties and microstructure of graphene nanoplatelet-cement composite. Nanomaterials 2016;6(11):200.
[16] Cao M-L, Zhang H-X, Zhang C. Effect of graphene on mechanical properties of cement mortars. J Central South Univ 2016;23:919–25.
[17] Tragazikis IK, Dassios KG, Exarchos DA, et al. Acoustic emission investigation of the mechanical performance of carbon nanotube-modified cement-based mortars. Constr Build Mater 2016;122:518–24.
[18] Metaxa Z. Polycarboxylate based superplasticizers as dispersant agents for exfoliated graphene nanoplatelets reinforcing cement based materials. J Eng Sci Technol Rev 2015;8(5):1–5.
[19] Dassios KG, Alafogianni P, Antiohos SK, et al. Optimization of sonication parameters for homogeneous surfactant-assisted dispersion of multiwalled carbon nanotubes in aqueous solutions. J Phys Chem C 2015;119(13):7506–16.
[20] Matikas TE. Towards the next generation of standards for service life of cement-based materials and structures. COST Action-TU1404; 2016.
[21] Aggelis DG, Soulioti DV, Sapouridis N, et al. Acoustic emission characterization of the fracture process in fibre reinforced concrete. Constr Build Mater 2011;25(11):4126–31.
[22] Hu Y, Luo D, Li P, Li Q, Sun G. Fracture toughness enhancement of cement paste with multi-walled carbon nanotubes. Constr Build Mater 2014;70:332–8.
[23] Tragazikis IK, Dassios KG, Exarchos DA, et al. Dramatic improvement of the fracture behaviour of cement mortars by carbon nanotubes [under review].
[24] Soulioti D, Barkoula NM, Paipetis A, et al. Acoustic emission behavior of steel fibre reinforced concrete under bending. Constr Build Mater 2009;23(12):3532–6.
[25] Papageorgiou DG, Kinloch IA, Young RJ. Mechanical properties of graphene and graphene-based nanocomposites. Prog Mater Sci 2017;90:75–127.